CHEMICAL ENGINEERING TRANSACTIONS
VOL. 57, 2017
A publication of AIDIC
The Italian Association of Chemical Engineering
Online at www.aidic.it/cet
Guest Editors: Sauro Pierucci, Jiří Jaromír Klemeš, Laura Piazza, Serafim Bakalis

ISBN 978-88-95608- 48-8; **ISSN** 2283-9216

Sensibility Analyses on Morphological Parameters of Cellulose Acetate - Graphene Oxide Nanocomposites using a Periodic 3D-FEM Model

Francesco Naddeo*, Lucia Baldino, Stefano Cardea, Alessandro Naddeo, Ernesto Reverchon

Department of Industrial Engineering, University of Salerno, Via Giovanni Paolo II, 132, 84084, Fisciano (SA), Italy
frnaddeo@unisa.it

This article focused on the study of the influence of morphological parameters on the mechanical performance (Young's modulus) of Cellulose Acetate-Graphene Oxide nanocomposites produced by Supercritical CO_2 assisted phase inversion, by means of an algorithm managing two parametric variational 3D finite element (FE) models simulating micro- and nano-level of the nanocomposite. Micro-level showed interconnected spherical pores, while nano-level showed a dispersion of not fully exfoliated graphene sheets. 3D FE model exploited the periodic representative volume element (PRVE) concept and accounted for the nanocomposite morphology as determined from Field Emission Scanning Electron Microscopy (FESEM) experiments. Model predictions were compared with experimental results obtained by compression tests at different weight percentages of graphene oxide with respect to the polymer. Once validated, such a FE simulation procedure allows to know in advance which and how to vary the geometrical parameters during the nanocomposite production to improve its final mechanical performance.

1. Introduction

Because of the difficulties in experimental investigation of nanostructured materials, analytical and numerical simulations are getting more attractive as alternatives. Analytical micromechanics theories such as Mori-Tanaka (Benveniste, 1987) and the Halpin-Tsai (Halpin, 1969) have been widely used (Chivrac et al, 2008) for the evaluation of composite materials properties, but they show documented limitations in the evaluation of the micro effects involved with individual fillers. In the field of modeling of elastic properties of composite structures, finite element (FE) method have been also widely used (Zeng, 2008) since it is possible more precisely to take into account adjacent fillers effects on the composite homogenized properties. Cricrì et al. (2012) recently compared 3D FE, Mori-Tanaka and experimental results conducted on nanocomposite films and concluded that FE estimations are reliable and promising. In particular, numerical tools enables to take into account the effects of different morphology parameters (the sheet interlayer spacing, the average number of sheet per stack, etc.), which cannot be directly accessed experimentally. Several attempts to model the effects of geometrical and material parameters on the elastic behavior of polymer-clay nanocomposites, have been already reported (Farnes and Paul, 2003; Van Es et al., 2001; Liu and Brinson, 2008; Figiel, Ł. and Buckley, 2009) and numerous complexities arise when comparing composite theory to experimental data. More recently, hierarchical modeling techniques take into account also the effect of the size and shape of the nanoparticles on the stiffness of polymer nanocomposites (Li et al., 2011). A better understanding of the influence of processing conditions on nanocomposite performances represents a key issue to facilitate the design and development of these systems. For this reason, is highly demanded by the industry.
This manuscript focuses on the modeling of the mechanical behavior of Cellulose Acetate (CA)-Graphene Oxide (GO) nanocomposite membranes. At this purpose, a 3D FE multiscale approach has been introduced. In the specific, a FE model representing the nanoscale has been realized by means of an original algorithm that generates the nanosheets position with the support of FESEM images. Periodic boundary conditions (PBC) and a PRVE sizing method were used to minimize the size of the model that gives acceptable scatter.

The GO particles were modeled as corrugated sheets, trying to pay attention to the spatial distribution and orientation; then, the homogenized results, in terms of elastic moduli, have been introduced in a PRVE representing the microscale modeled in the FE environment as a close-packing of equal spheres based on the theory of hexagonal close-packed (hcp). Finally, FE results have been compared with experimental results and a very good matching has been achieved confirming the validity of the reported FE procedure.

2. Materials and methods

Cellulose acetate, CA, (average Mn ca. 50 000 with acetyl content of 39.7 %), N-Methylpyrrolidine, NMP, (purity 99.7 %) and Graphene Oxide powder, GO, (bulk density ~1.8 g/cm^3) were bought from Sigma-Aldrich. CO_2 (99.5 % purity) was supplied by Morlando Group S.R.L. (Sant'Antimo, NA - Italy). All materials were used as received.

2.1 Preparation, characterization and properties of the nanocomposite

CA/GO nanocomposites were produced by a supercritical CO_2 (SC-CO_2) assisted phase inversion process (Cardea et al., 2014; De Marco et al., 2014; Baldino et al., 2016). Solutions of CA in NMP with a concentration of 25 % w/w were prepared. Subsequently, GO was suspended in the polymeric solution at different concentrations: 3 % w/w and 9 % w/w with respect to the polymer. Then, the suspension was spread on steel caps inside an high pressure vessel and phase separated using supercritical CO_2 (SC-CO_2) for 4 h, at 200 bar and 40 °C, with a CO_2 flow rate of about 1.5 Kg/h. Other details about the supercritical process can be found in a previous work on CA/GO nanocomposite production (Baldino et al., 2015a). CA/GO nanocomposites were cryofractured using liquid Nitrogen; then, the samples were sputter coated with Gold (Agar Auto Sputter Coater mod. 108 A, Stansted, UK) at 30 mA for 160 s and were analyzed by FESEM (mod. LEO 1525, Carl Zeiss SMT AG, Oberkochen, Germany) to check the pore size and the overall structure morphology.
Sigma Scan Pro 5.0 (Jandel Scientific, San Rafael, CANADA) and Origin 8.5 (Microcal, Northampton, USA) were used to determine the average diameter of the pores in the structure. Images taken at various locations in the structure were used for each calculation. We measured about 300 pores for each sample analyzed. Using Origin software, we first represented a histogram with the percentage of the pores having a given diameter; then, we performed a curve fitting to obtain the distribution curve. A quasi-constant overall porosity (between 80 and 82 %) of the samples was also measured. Compressive mechanical properties of the nanocomposites were measured using an INSTRON 4301 (Instron Int. Ltd, High Wycombe, UK). Cylindrical samples with a diameter of 2 cm and a mean thickness of 4 mm were compressed at a cross-head speed of 1 mm/min. The compressive modulus is defined through the shape of the initial linear portion of the stress-strain curve. Five specimens were tested for each sample.
The CA/GO nanocomposite showed in all cases a porous morphology, as the one reported in Figure 1.

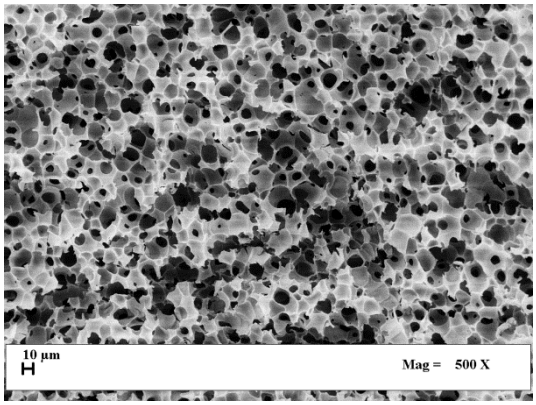

Figure 1: Example of CA/GO nanocomposite morphology.

The mean pore size was: 9.7 ± 2.4 µm and 15.2 ± 3.9 µm for the CA membranes loaded at 3 % w/w GO and 9 % w/w GO, respectively.
The Young modulus of CA membrane was around 123 ± 20 MPa; whereas, the Young modulus of CA/GO 3 % w/w and CA/GO 9 % w/w was 327 ± 31 and 549 ± 53 MPa, respectively.

2.2 FE modeling

Modeling the micrometric porous structure

By using Ansys FE simulation environment, an algorithm has been written that, depending on the porosity, realizes a porous hexagonal prism-shaped PRVE, based on the theory of hcp (Baldino et al.,2015b; Naddeo et al., 2016) (see Figure 2). This shape has been chosen because the linear elastic behaviour and micromorphology is very well approximated.

We can easily calculate the homogenized Young's modulus along the axis of the prism, using the following relationship:

$$E_{xx} = \frac{\langle \sigma_{xx} \rangle}{\langle \varepsilon_{xx} \rangle} \tag{1}$$

$\langle \varepsilon_{xx} \rangle$ being the strain component applied to the PRVE in the *x* direction; and

$$\langle \sigma_{xx} \rangle = \frac{\sum \sigma_{xxi} v_i}{V_p} \tag{2}$$

in which σ_{xxi} is the *x* normal component of the Cauchy Tensor and v_i the volume of the i-th finite element of the model; V_p the volume of the pore-free virtual hexagonal prismatic PRVE.

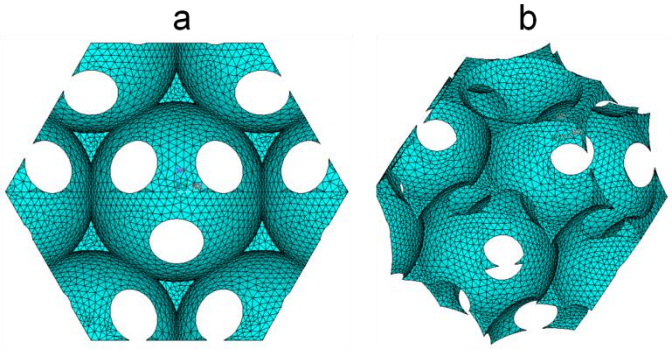

Figure 2: PRVE FE model (micrometric structural level): a) Top view; b) 3D view.

Modeling the nanometric structure

By means of a semi-automatic FESEM image analysis (Cricrì et al., 2012), we realized that the particles (modeled as square sheets) arranged themselves substantially in a random way (orientation and position). An average percentage of intercalated clusters were evaluated equal to 10 % and an average spacing of 5 nm was measured. An average number of sheets per cluster of 3 was measured and introduced in the virtual model. For this work, we used an original parameterized Random Sequential Adsorption Algorithm (RSAA) that creates an easily manageable parametric FE model, which has all the information concerning with the morphology of the hybrids and the mechanical properties of the composite phases. The nanocomposite systems were represented by a periodic distribution of sheets in an infinite matrix. As repetitive cell of this distribution, we have chosen a reasonably small cubic-shaped portion of space (PRVE), to minimize FE runs' computational times. The RSAA shows some very well documented limits (Jamming limit) (Viot et al., 1992). These limits are related to the inability to go beyond a certain threshold of the volume fraction of filler (GO). This value decreases with decreasing aspect ratio of the filler sheets. For this reason, in this work we have decided to model only the sample loaded at 3 % w/w GO, which is characterized by a lower volume fraction.

The nanosheets were modeled as square sheets, whose geometric parameters' values were mediated from those extrapolated by FESEM image analysis (see Figure 3a). The centroids and the orientations of the square sheets were randomly generated. For all simulations, a sequential generation of square sheets was performed imposing two conditions: 1) generated nanosheets must not overlap each other within the domain; 2) parts of the nanosheets that intersect the outline and so lie partly outside the PRVE, must be included in the PRVE on the opposite side of the boundary. This arrangement was used to obtain a FE model with geometrical periodicity that allows the implementation of the PBC (Hori and Menat-Nasser, 1999) to extrapolate the mechanical properties more accurately. The square sheets were assumed to be perfectly bonded to the polymer matrix and therefore, merged with the matrix during the realization of the FE model (see Figure 3b). A convergence analysis of the results (in terms of mechanical properties) was realized.

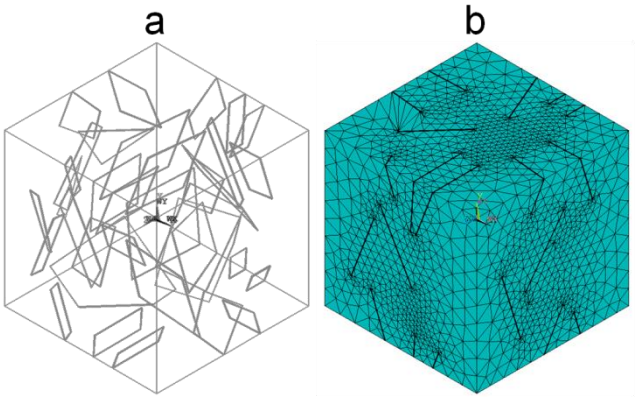

Figure 3: PRVE modeling the nanometric structure: a) 3D wireframe geometry; b) 3D FE model.

An *ad hoc* written FE routine was used for creating an identical surface distribution of nodes on the opposite sides (Naddeo et al., 2014) in order to apply displacement which can be expressed in the following synthetic matrix form:

$$u_2 - u_1 = \varepsilon(X_2 - X_1) \tag{3}$$

With ε, being the *strain tensor*, X_i (i = 1, 2) being the position vector of the points belonging to opposite sides of the PRVE and u_i being the relative displacement. For each simulation, this routine performed three virtual static tensile tests and three static shear tests (with imposed average strains) in order to have an exhaustive representation of the mechanical behavior of the structure. Imposing the overall strain to the PRVE: $\langle\varepsilon\rangle = [0 \dots \langle\varepsilon_i\rangle \dots 0]$ and assuming elastic behaviour and small strains of the material, for each i-th imposed strain, the routine allowed for calculating all the components of the corresponding i-th column of the stiffness matrix using the following formulation (elastic overall constitutive law):

$$\overline{C_{hi}} = \frac{\langle\sigma_h\rangle}{\langle\varepsilon_i\rangle} \tag{4}$$

$\forall\, h$, i = 1,...,6, with $\langle\sigma_h\rangle$ being the stress component calculated in the FE post-processing environment, using the following relation:

$$\langle\sigma_h\rangle = \frac{\sum_{elem} \sigma_{h_{elem}} vol_{elem}}{vol_{RVE}} \tag{5}$$

$\sigma_{h_{elem}}$ being the *h-th* stress component of the single finite element, due to the *i-th* imposed strain, vol_{elem} being the element volume and vol_{RVE} the volume of the PRVE. In this way, the routine calculated all the components of the stiffness matrix with Eq(4) by means of a single FE run, characterized by six sequential imposed strains. Finally, the routine automatically provided the stiffness and compliance matrices of the examined cubic PRVE in output. The PRVE size influences the simulation computational effort and the possibility that the nanosheets distribution can be distorted (the position of a sheets may affect the position of the sheets generated later). For this reason, intrinsic statistical characteristics were taken into consideration when choosing the PRVE size in order to obtain an acceptable starting isotropic degree. An original isotropic criterion (Cricrì et al., 2012) to optimize the size of the cubic PRVE was implemented.

3. Results

3.1 FE modeling results and improvements by means of parameterization

As reported in paragraph 2.2, we approximated the micrometric structure to a “close-packaging of equal spheres” (Figure 2) obtaining a homogenized resulting Young’s modulus equal to about 5 % of the Young’s modulus introduced as input, the porosity being set at the experimental value of about 82 %. Therefore, by introducing as input the Young’s modulus of the neat CA equal to E_{CA} = 2400 MPa and a Poisson ratio equal to v_{CA} = 0.3827 (Azom, 2016) in the micrometric PRVE, we obtained a homogenized numerical value of the Young’s modulus, representative of the microporous structure, equal to E_{FE_CA} = 119.21 MPa. This Young’s modulus value is fairly close to the one experimentally obtained (E_{ex} = 123 ± 20 MPa). Then, introducing in the nanometric PRVE a Young’s modulus of GO equal to E_{GO} = 425 GPa and a Poisson’s ratio of GO equal to v_{GO}

= 0.197 (Nikolaou et al., 2016), we obtained a homogenized Young's modulus, corresponding to CA/GO 3 % w/w, equal to $E_{FE\_CA\_GO}$ = 5050 MPa. This value was averaged among those calculated in the three mutual perpendicular directions of the cubic PRVE after reaching a good degree of isotropy (see section 2.2). This numerical value, representing the nanocomposite CA/GO, has been introduced in the micrometric PRVE in order to evaluate numerically the effect of the micrometric pores on the mechanical behavior of the nanocomposite in terms of Young's modulus, obtaining $E_{FE\_CA\_GO}$ = 355 MPa. This result slightly overestimates the experimental one (327 ± 31). This phenomenon can be easily explained considering that the GO sheets actually exhibit a rough surface showing wrinkles. It is possible to demonstrate that particles having this shape tend to behave like flexible elements (springs) reducing the overall structural rigidity of the nanocomposite (Shen et al., 2014). This leads to a reduction of the homogenized Young's modulus. For this reason, on the bases of FESEM image analysis, the algorithm versatility allowed us to easily introduce wrinkles in the nanosheets by modeling them as sheets having a corrugate profile (see Figure 4b). Furthermore, a sensitivity analysis has been done, number of corrugation (5 for each sheet) and volume fraction being equal, varying the corrugation angle and keeping the sheets aspect ratio in a fairly narrow neighborhood of the average experimental value. In correspondence of a corrugation angle equal to α = 120° (see Figure 4c) we have obtained as result a homogenized Young's modulus of $E_{FE\_CA\_GO}$ = 332.00 MPa, very close to the experimental one (327 ± 31). Table 1 shows the comparison between experimental and numerical results in terms of Young's modulus.

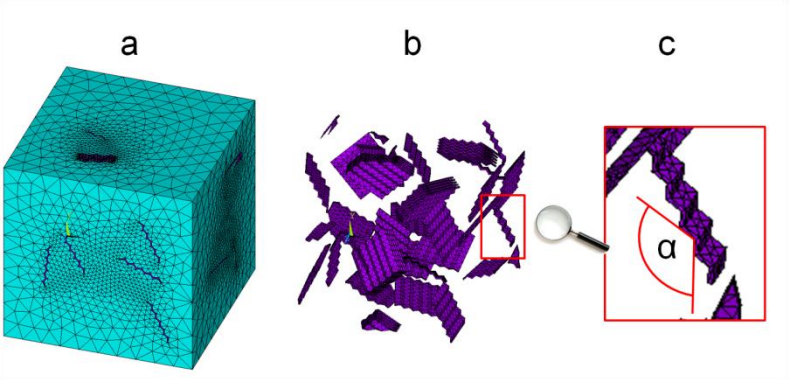

Figure 4: FE model: a) polymer matrix and corrugated GO sheets; b) isolated corrugated GO sheets; c) corrugation angle.

Table 1: Comparison between experimental and numerical results

Young's modulus	Experimental (MPa)	FE (MPa)
CA	123 ± 20	119
CA/GO 3 % w/w	327 ± 31	332

4. Discussion, conclusions and perspectives

This work was focused on the FE modeling of mechanical behavior of CA/GO nanocomposite membranes produced by SC-CO_2 assisted phase inversion. Comparison between numerical and experimental results, has confirmed the reliability of the numerical procedure used in this study that reached a good approximation of the experimental trend. Numerical results slightly overestimate experimental results once sheets are considered as flat particles. This phenomenon can be easily explained considering that the GO sheets actually exhibit a rough surface showing wrinkles tending to reduce the overall structural rigidity of the nanocomposite. This leads to a reduction of the homogenized Young's moduli. Moreover, the nanosheets were assumed to be perfectly bonded to the polymer matrix without consider any kind of different interaction between mutual surfaces, increasing the structural stiffness of the composite. For simulating the behavior of the sheets induced by wrinkles, we have introduced a corrugated profile for the sheets obtaining a very good matching of the experimental results. At this point, it is worthy to point out the potentialities of a FE-based micro/nano mechanical approach carried on by a fully parameterized algorithm able to easily take into account of different statistical, morphometric and material-related aspects.

In perspective, the idea is to use this procedure as a tool to understand/confirm the interactions among different phases or to predict how optimized structures can be obtained. Possible future developments of the proposed procedure may be:

1) modeling the behavior at the nanosheets/matrix interface, in order to properly analyze the mechanisms of fracture for these systems (that can be obtained by integrating the FE models with molecular dynamics to better characterize the atomistic effects at interface GO/CA);
2) the evaluation of the effect of large deformations and the implementation of new material characteristics to cover the field of geometrical and material nonlinearity.

References

AZO Materials, 2002, Cellulose Acetate <www.azom.com> accessed 21.12.2016.

Baldino L., Cardea S., Reverchon E., 2016, Production of antimicrobial membranes loaded with potassium sorbate using a supercritical phase separation process, Innovative Food Sci. Emerging Technol. 34, 77-85.

Baldino L., Concilio S., Cardea S., De Marco I., Reverchon E., 2015a, Complete glutaraldehyde elimination during chitosan hydrogel drying by SC-CO2 processing, J. Supercrit. Fluids 103, 70-76.

Baldino L., Naddeo F., Cardea S., Naddeo A., Reverchon E., 2015b, FEM modeling of the reinforcement mechanism of Hydroxyapatite in PLLA scaffolds produced by supercritical drying for Tissue Engineering applications, J. Mech. Behav. Biomed. Mater. 51, 225–236.

Benveniste Y., 1987, A new approach to the application of Mori-Tanaka's theory in composite materials, Mech. Mater. 6, 147-57.

Cardea S., Baldino L., De Marco I., Reverchon E., 2014, Generation of loaded pmma scaffolds using supercritical CO2 assisted phase separation, Chem. Eng. Trans. 38, 241-246.

Chivrac F., Gueguen O., Pollet E., Ahzi S., Makradi A., Averous L., 2008, Micromechanical modeling and characterization of the effective properties in starch-based nano-biocomposites, Acta Biomater. 4, 1707-1714.

Cricrì, G., Garofalo, E., Naddeo, F., Incarnato, L., 2012, Stiffness constants prediction of nanocomposites using a periodic 3D FEM model, J. Polym. Sci., Part B: Polym. Phys. 50, 207-220.

De Marco I., Baldino L., Cardea S., Reverchon E., 2014, Production of ethyl cellulose scaffolds by supercritical co2 phase separation, Chem. Eng. Trans. 38, 265-270.

Figiel Ł., Buckley C.P., 2009, Elastic constants for an intercalated layered-silicate/polymer nanocomposite using the effective particle concept – A parametric study using numerical and analytical continuum approaches, Comput. Mater. Sci. 44, 1332–1343.

Halpin J.C., 1969, Stiffness and Expansion Estimates for Oriented Short Fiber Composites, J. Compos. Mater. 3, 732-734.

Hori M., Nemat-Nasser, 1999, On two micromechanics theories for determining micro-macro relations in heterogeneous solid, S. Mech. Mater. 31, 667–682.

Li Y., Waas A. M., Arruda E.M., 2011, A closed-form, hierarchical, multi-interphase model for composites—Derivation, verification and application to nanocomposites, J. Mech. Phys. Solids 59, 43–63.

Liu H., Brinson L.C., 2008, Reinforcing efficiency of nanoparticles: A simple comparison for polymer nanocomposites, Compos. Sci. Technol. 68, 1502–1512.

Naddeo F., Baldino L., Cardea S., Naddeo A., Reverchon E., 2016, Optimization of an ad hoc realized lattice structure structured RVE for FEM modeling of nanoporous biopolymeric scaffolds obtained by supercritical fluids assisted process, Chem. Eng. Trans. 49, 169-174.

Naddeo F., Cappetti N., Naddeo A., 2014, Automatic versatile parametric procedure for a complete FEM structural analysis of composites having cylinder-shaped reinforcing fibres, Comput. Mater. Sci. 81, 239-245.

Nikolaou I., Hallil H., Conedera V., Plano B., Tamarin O., Lachaud J.-L., Talaga D., Bonhommeau S., Dejous C., Rebiere D., 2016, Electro-mechanical properties of inkjet-printed graphene oxide nanosheets, Phys. Status Solidi A, DOI: 10.1002/pssa.201600492.

Shen X., Lin X., Yousefi N., Jia J., Kim J.K., 2014, Wrinkling in graphene sheets and graphene oxide papers, Carbon 66, 84–92.

Van Es M., Xiqiao F., van Turnhout J., Van der Giessen E., 2001, Comparing polymer-clay nanocomposites with convential composites using composite modeling. In S Al-Malaika, A Golovoy & CA Wilkie (Eds.), Speciality Polymer Additives - Principles and Applications, 391-413. Oxford: Blackwell science.

Viot P., Tarjus G., Ricci S., Talbot J., 1992, Random sequential adsorption of anisotropic particles. I. Jamming limit and asymptotic behaviour, J. Chem. Phys. 97, 5212.

Zeng Q.H., Yu A.B., Lu G.Q., 2008, Multiscale modeling and simulation of polymer nanocomposites, Prog. Polym. Sci. 33, 191-269.